Contents lists available at ScienceDirect

# Carbohydrate Polymers

# Chemical treatment and characterization of soybean straw and soybean protein isolate/straw composite films

Milena Martelli-Tosi [a,b,*], Odílio B.G. Assis [c], Natália C. Silva [a], Bruno S. Esposto [a],
Maria Alice Martins [c], Delia R. Tapia-Blácido [a]

[a] *Departamento de Química, Faculdade de Filosofia, Ciências e Letras de Ribeirão Preto, Universidade de São Paulo, Bandeirantes Avenue 3900, CEP 14040-901, Ribeirão Preto, SP, Brazil*
[b] *Departamento de Engenharia de Alimentos, Faculdade de Zootecnia e Engenharia de Alimentos, Universidade de São Paulo, Rua Duque de Caxias Norte 225, CEP 13635-900, Pirassununga, SP, Brazil*
[c] *Embrapa Instrumentação, National Nanotechnology Laboratory for Agriculture, Rua XV de Novembro, 1452, CEP 13561-206, São Carlos, SP, Brazil*

## ABSTRACT

This work investigated changes in the chemical composition and structure of soybean straw (SS) treated with alkali (NaOH 5% and 17.5%) and bleached with hydrogen peroxide ($H_2O_2$) or sodium hypochlorite (NaOCl). Removal of the amorphous constituents increased the degree of crystallinity and the content of cellulose fibers particularly after reaction with high concentrations of alkali. Treatment with NaOH 17.5% contributed to the allomorph transition from cellulose I to II regardless of the bleaching agent, but $H_2O_2$ as bleaching agent promoted more effective delignification. This work also evaluated the potential use of treated and non-treated SS as reinforcement filler in soy protein isolate film (SPI). Films added with treated SS presented higher mechanical resistance, lower elongation at break, and lower solubility in water. Addition of non-treated SS did not affect the properties of the SPI film significantly. The low solubility and the reasonable water vapor permeability of the composite films make them suitable packaging materials for fresh fruit and vegetables.

© 2016 Elsevier Ltd. All rights reserved.

## 1. Introduction

Soybean is a significant agricultural commodity in the Brazilian economy (Milazzo, Spina, Cavallaro, & Bart, 2013). The 2015/2016 harvest placed Brazil as the second largest world producer of soybean (about 30% of the global production) (CONAB, 2015). Unfortunately, grain threshing generates a huge amount of soybean straw. According to Bose and Martins Filho (1984), the soybean/straw ratio statistically varies from 1:1.2 to 1:1.5 t/ha, which means that about 104 to 130 million tons/year of straw originates from the Brazilian soybean harvest alone (FAOSTAT, 2016). The soybean straw consists of stems, leaves, and pods. The average composition of this material includes 35% cellulose, 21% insoluble lignin, 17% hemicelluloses, 11% ash, 1% acid soluble lignin, and remaining constituents such as protein, pectin, and glucuronic acid

substitutes (Cabrera et al., 2015; Wan, Zhou, & Li, 2011). Soybean straw is usually disposed as waste through landfilling, incineration, or dumping.

Some studies have suggested that soybean straw could be used as raw material to produce polymer and soluble sugars (Cabrera et al., 2015; Wan et al., 2011; Xu, Wang, Jiang, Yang, & Ji, 2007) or as a natural source to obtain fibers via alkali and acid treatments (Reddy & Yang, 2009).

Various physical, chemical, and enzymatic treatments can enhance the biodegradability and digestibility of soybean straw (Cabrera et al., 2015; Khorvas, Kargar, Yalchi, & Ghorbani, 2010). Application of chemical treatments before enzymatic hydrolysis removes amorphous components like lignin and hemicellulose, thereby increasing the porosity of the material and facilitating further defibrillation and extraction of fibers (Yue et al., 2015). Chemical treatments include reactions with ozone, alkali, acid, peroxide, or other organic solvents (Oh et al., 2015). The pulp industry has traditionally delignified lignocellulose via bleaching with sodium chlorite. However, environmental concerns have led the industry to replace bleaching with sodium chlorite with more environmentally friendly methods such as thermochemical reac-

* Corresponding author at: Departamento de Engenharia de Alimentos, Faculdade de Zootecnia e Engenharia de Alimentos, Universidade de São Paulo, Av. Duque de Caxias Norte 225, CEP 13635-900, Pirassununga, SP, Brazil.
*E-mail address:* mmartelli@usp.br (M. Martelli-Tosi).

tions that use oxygen (Kafle et al., 2015) and hydrogen peroxide (Andrade-Mahecha, Pelissari, Tapia-Blácido, & Menegalli, 2015; Zeronian & Inglesby, 1995). According to Khorvash et al. (2010), treatment with $H_2O_2$ improves the *in vitro* digestibility of soybean straw as compared to $NaClO_2$-based treatments. Depending on the size of the generated soybean fibers, they can serve as reinforcement fillers during formation of biocomposite matrixes.

Biomaterials based on renewable resources, such as proteins and polysaccharides, can be potentially processed into films for food or biomedical applications. In particular, soy protein isolate (SPI), which can be produced by casting (Denavi et al., 2009), extrusion, or injection molding (Calabria et al., 2012; Chan, Lim, Barbut, & Marcone, 2014; Garrido, Peñalba, de la Caba, & Guerrero, 2016), is an attractive sustainable "green polymer" with good film-forming ability. Nevertheless, SPI films have low strength and absorb a high amount of moisture, which limits their applications. Three methods can help to overcome these limitations and to improve the properties of SPI films, namely cross-linking (González, Strumia, & Alvarez Igarzabal, 2011; Xu et al., 2015), blending with a polymer to form a soy-based plastic (Calabria et al., 2012; Kim & Netravali, 2012; Saenghirunwattana, Noomhorm, & Rungsardthong, 2014; Won, Lee, Jin, & Lee, 2015), and addition of reinforcing fillers (Husseinsyah, Yeng, Kassim, Zakaria, & Ismail, 2014; Lodha & Netravali, 2002; Siro & Plackett, 2010).

Micro- and nanosized fibers have by far been the most cited reinforcement fillers in the literature (Chan et al., 2014; Chen, Zhang, Peng, & Liao, 2006; Jensen, Lim, Barbut, & Marcone, 2015; Saenghirunwattana et al., 2014; Satyanarayana, Arizaga, & Wypych, 2009; Wang, Cao, & Zhang, 2006; Wei, Fan, Huang, & Chen, 2006). Hydrophobic and electrostatic interactions are the driving forces behind the establishment of a network between fibers and proteins; these interactions improve the mechanical and water resistance properties of composite films (Jensen et al., 2015; Sun, Chen, Liu, Li, & Yu, 2015; Saenghirunwattana et al., 2014; Wang et al., 2006). There are few reports on the characterization and use of chemically treated soybean straw as reinforcing filler in SPI films.

The present study aimed to evaluate (1) how four different sequences of chemical treatment with alkali and bleaching affect the structure and composition of the soybean straw and (2) how the incorporation of treated fibers as reinforcing fillers into soy protein films influences the mechanical and permeability properties of the resulting film.

## 2. Materials and methods

### 2.1. Materials

Soybean straw was provided by Embrapa Soja (Londrina, Brazil). The residues were washed with distilled water and dried at 50 °C for 72 h in an oven with forced circulation (Q314M, Quimis, Brazil). The dried samples were then ground in a knife mill SL31 (Solab, Brazil) and sieved through 100-mesh sieves (Tyler series, 150 μm).

Solae® (Brazil) supplied the soy protein isolate (SPI). Glycerol was purchased from Sigma-Aldrich (Saint Louis, USP). Chemicals were obtained from Labsynth (Diadema, Brazil) (NaOH, $NaClO_2$ and $H_2O_2$) and Dinâmica (Diadema, Brazil) ($CH_3COOH$ and $MgSO_4·7H_2O$).

### 2.2. Chemical treatments of soybean straw

The soybean straw particles underwent four different chemical treatments, including treatment with alkali followed by a bleaching step. The concentrations of alkali and $H_2O_2$ and the temperature used during the treatments were based on previous results obtained for the treatment of achira fibers (Andrade-Mahecha et al.,

2015). The conditions of the bleaching reaction involving $NaClO_2$ were the same as the conditions described by Campos et al. (2013). Fig. 1 summarizes the sequence of these treatments. According to the intensity of the reaction, the treatments were denoted severe or mild as follows:

(i) Severe: NaOH at 5% (T1) or 17.5% (T2) (w/v) at 90 °C for 1 h, repeated twice. The solution was brought to room temperature and rinsed to neutralization. The fibers were then bleached with aqueous 0.7% acetic acid and 3.3% sodium chlorite ($NaClO_2$) solution under agitation at 75 °C for 3 h.

(ii) Mild: NaOH at 5% (T3) or 17.5% (T4) (w/v) at 30 °C for 15 h. After this period, the solution was brought to room temperature and rinsed to neutralization. The resulting fibers were bleached in a mixture of 4% $H_2O_2$ (w/v) and 2% NaOH (w/v) at 90 °C for 3 h. $MgSO_4·7H_2O$ at 0.3% (w/v) was added as stabilizer. The solution was cooled to room temperature, and the fibers were filtered and washed with distilled water until neutral pH was achieved, followed by rinsing with ethanol and acetone. The final fibers were dried at 50 °C in an oven with air circulation.

### 2.3. Characterization of soybean straw

#### 2.3.1. Chemical composition

Analysis of the cellulose, holocellulose (cellulose + hemicelluloses), and lignin content in the soybean straw was carried out before and after each treatment. The procedures were performed according to TAPPI T19 om-54 (TAPPI, 1991), TAPPI T 222 om-22 (TAPPI, 1999), and the methodology presented by Sun (2004).

#### 2.3.2. Particle size distribution

The particle size distribution of untreated and chemically treated soybean straw was measured with a Beckman Coulter LS 13320 Laser Diffraction Particle Size Analyzer (Beckman Coulter, Miami, FL, USA). To this end, the powdered samples were sieved through 100-mesh sieves (Tyler series, 150 μm) and dispersed in ethanol under sonication for 5 min. The mean particle size and standard deviation (SD) were calculated by using the Beckman Couter software.

#### 2.3.3. Scanning electron microscopy (SEM)

Soybean straw samples were mounted on aluminum stubs and coated with gold in a Bal-Tec SCD 050 sputtering system (Balzers, Liechtenstein). Images were obtained in a Zeiss EVO 50 (Cambridge, UK) scanning electron microscope at an accelerating voltage of 20 kV.

#### 2.3.4. X-ray diffraction (XRD)

The effect of chemical treatment on the crystallinity of soybean straw was determined in a Shimadzu X-ray Diffractometer XRD-6000 (Shimadzu, Japan) with Cu kα radiation, at 30-kV voltage and 30-mA tube current. The measurements were carried out for $2\theta$ values ranging from 5 to 40°, at a scan rate of 1° min$^{-1}$. To calculate the crystallinity index ($I_{cr}$) two different methods were used. One method consisted of estimating $I_{cr(S)}$ according to the Segal, Creely, Martin, and Conrad (1959) relation:

$$I_{cr(S)} = \frac{I_{002} - I_{am}}{I_{002}} x100 \tag{1}$$

where $I_{002}$ is the intensity of the 002 lattice diffraction at $2\theta = 22.8°$ (crystalline contribution), and $I_{am}$ is the intensity of the diffraction at $2\theta = 18°$ considering the amorphous diffraction. The other method uses a curve-fitting process to estimate individual crystalline peaks from the intensity of the diffraction profiles after subtraction of the baseline spectrum. The Origin 9.0 software was
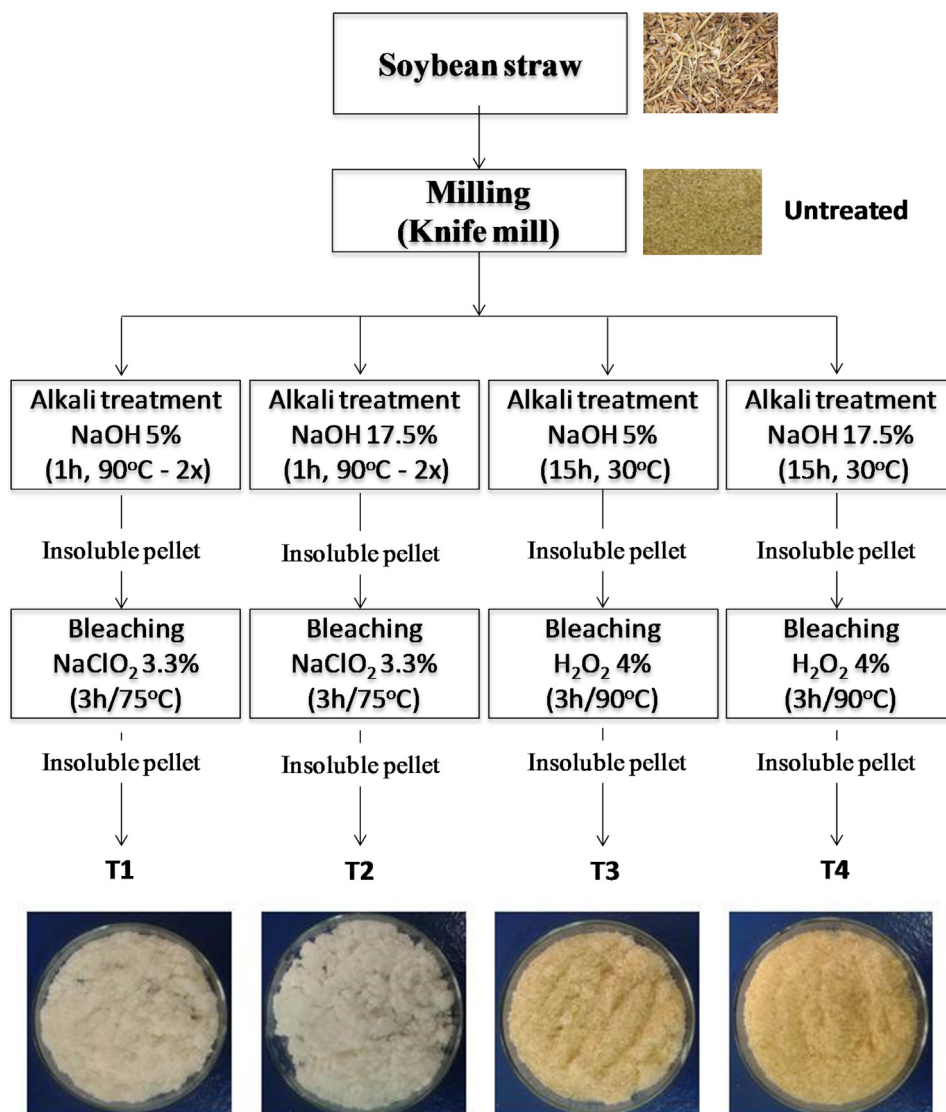
**Fig. 1.** Chemical pre-treatments of the soybean straw.

used, and Gaussian functions were fitted for each peak. The broad peak around 21.5° was assigned to amorphous contribution (Park, Baker, Himmel, Parilla, & Johnson, 2010). $I_{cr(D)}$ was calculated by dividing the area under the peaks due to crystalline cellulose I and II by the total area of the original diffractogram.

### 2.3.5. Thermogravimetric analyzer (TGA)

The thermal properties of untreated and treated soybean straw were evaluated on a Thermogravimetric Analyzer TGA-Q500 (TA Instruments, USA). Approximately 10 mg of each sample was weighed in platinum pans. The studied temperature range was 25–700 °C; the heating rate was 10 °C/min, under nitrogen atmosphere. Mass changes were continuously recorded as a function of temperature.

### 2.3.6. Attenuated total reflection Fourier transform infrared spectroscopy (ATR-FTIR)

Untreated and treated soybean straw samples were analyzed by Attenuated Total Reflection Fourier Transform Infrared Spectroscopy (ATR-FTIR) (IR Prestige-21, Shimadzu, Japan) to identify the functional groups in the fiber and any chemical changes that may have occurred in the polymeric structure. All the spectra were

the average of 40 scans recorded at a resolution of $2\,cm^{-1}$ from $4000\,cm^{-1}$ to $400\,cm^{-1}$.

### 2.4. Preparation of SPI/soybean straw composite films

Untreated and treated soybean straw samples were sieved through 100-mesh sieves (Tyler series, 150 μm) and re-suspended in water 24 h before film processing. The composite films were prepared from an aqueous soy protein isolate suspension at 5% w/w, homogenized in an Ultra-Turrax homogenizer (model Q252-28, Quimis, Brazil) for 2 min, and heated at 40 °C for 20 min under mechanical agitation in a thermostatic bath. Glycerol (25 g) was added as plasticizer along with 1 g of untreated or chemically treated soybean straw as reinforcing filler to every 100 g of SPI. The pH was adjusted to 10.5 with NaOH 1 M, and the fibers were kept under mechanical agitation at 40 °C for 10 min. The solutions were placed in ultrasonic bath (USC 1400, Unique, Brazil) for 2 min, poured on the acrylic plates, and dried in a BOD incubator (SL 200/364U, Solab Cientifica, Brazil) at 30 °C and 58% relative humidity for 24 h. Before characterization, all the films were pre-conditioned for at least 72 h in desiccators containing saturated NaBr solution (58% RH).

**Table 1**
Particle size and chemical composition of untreated and chemically treated soybean straw.

| Treatment | Particle Size (μm) | Cellulose (%) | Hemicelluloses (%) | Insoluble Lignin (%) | Soluble Lignin (%) |
|---|---|---|---|---|---|
| Untreated | $116 \pm 73^a$ | $39.8 \pm 0.6^c$ | $22.6 \pm 1.0^a$ | $10.5 \pm 0.7^a$ | $2.31 \pm 0.18^a$ |
| T1 | $108 \pm 78^a$ | $62.9 \pm 0.6^b$ | $11.1 \pm 0.1^b$ | $4.9 \pm 0.2^b$ | $1.42 \pm 0.09^b$ |
| T2 | $88 \pm 71^a$ | $67.1 \pm 0.2^a$ | $9.8 \pm 0.4^b$ | $4.1 \pm 0.2^{bc}$ | $1.51 \pm 0.04^b$ |
| T3 | $145 \pm 106^a$ | $64.0 \pm 0.7^b$ | $10.7 \pm 0.1^b$ | $3.6 \pm 0.1^c$ | $0.67 \pm 0.02^c$ |
| T4 | $122 \pm 79^a$ | $66.2 \pm 0.5^a$ | $9.5 \pm 1.1^b$ | $3.5 \pm 0.1^c$ | $0.73 \pm 0.09^c$ |

[a–d] Means with different superscript letters in the same column are statistically different at $p < 0.05$ according to the Tukey's test.

## 2.5. Characterization of SPI/soybean straw composite films

### 2.5.1. Mechanical properties

The mechanical tests were performed on a texture analyzer TA TX Plus (TA Instrument, England). The tensile strength (TS) and elongation at break (EB) were obtained according to the ASTM D882-95 method (ASTM D882-95, 1995), taking an average of five determinations in each case. Sample films were cut into 2.54-cm-wide strips with a length of at least 10 cm. The initial grip separation and the crosshead speed were set at 80 mm and 1.0 mm s$^{-1}$, respectively. Young's modulus (YM) was calculated as the inclination of the initial linear portion of the stress versus strain curve by using the Texture Expert V.1.22 (SMS) software.

### 2.5.2. Solubility in water, moisture, and water vapor permeability (WVP)

The solubility in water was calculated as the percentage of dry matter of the solubilized film after immersion of three previously weighed samples (discs with 20 mm of diameter) for 24 h in 50 mL of water at $25 \pm 2\,°C$, under mechanical stirring. This was followed by a procedure described by Tapia-Blácido, Sobral, and Menegalli (2011). Sodium azide (0.02% w/v) was added to prevent microbial growth. The remaining non-solubble matter was filtered through qualitative filter paper (80 g m$^{-3}$) and dried at 50 °C until constant weight was achieved. The moisture content in the films was also determined by drying the materials in an oven at 105 °C until constant weight ($\sim$24 h), and the water vapor permeability (WVP) test was performed by using a modified ASTM Standard method (ASTM E96-95, 1995) at $25 \pm 2\,°C$. Film samples were sealed over the circular opening of a permeation cell containing silica gel, and the cells were then placed in desiccators containing distilled water. After the samples had reached steady-state conditions ($\sim$20 h), the cell was weighed every 1 h for 9 h on an analytical scale. WVP was calculated as WVP = $w.x/t.A.\Delta P$, where "x" was the average thickness of the films, "A" was the permeation area (0.00196 m$^2$), "$\Delta P$" was the difference between the partial pressure of the atmosphere over silica gel and over pure water (3.168 kPa, at 25 °C), and the term w/t was calculated by linear regression from data of weight gain as a function of time. The solubility in water, WVP, and moisture content were analyzed in triplicate.

### 2.6. Statistical analyses

Experimental data were statistically evaluated by Fisher or Tukey's test with significance set at $p < 0.05$. The software Statistica7.0 (StatSoftInc, Tulsa, USA) was employed.

## 3. Results and discussion

### 3.1. Chemical treatment of soybean straw

#### 3.1.1. Chemical composition

The untreated soybean straw contained 39.8% cellulose, 2.3% soluble lignin, 10.5% insoluble lignin, and 22.6% polysaccharides, including hemicelluloses, which agreed with values reported in the literature (Wang, Mo, Sun, & Wang, 2007). The lignin and hemicelluloses contents decreased and the cellulose fraction increased after the chemical treatments (Table 1).

Treatments with high concentration of NaOH (17.5%) and bleaching with NaClO₂ or H₂O₂ (T2 and T4) yielded samples with high cellulose and low hemicelluloses and lignin content regardless of the treatment conditions (severe or mild). Several authors have reported that basic conditions (alkali treatment) favor the removal of hemicelluloses due to cleavage of the ester-linked substances (Deepa et al., 2011; Kallel et al., 2016; Xiao, Sun, & Sun, 2001). Kallel et al. (2016) also observed that the lignin content in the fibers of garlic straw remained practically constant after alkali treatment. To remove the lignin residues, the authors conducted bleaching with sodium chloride, which resulted in almost pure cellulose fibers. In our study, bleaching with H₂O₂ (T3 and T4) generated fibers with slight superior delignification as compared to bleaching with sodium chloride. The fraction of acid-insoluble lignin decreased from 10.5% to 3.6 and 3.5%, respectively, while soluble lignin reduced from 2.3% to approximately 0.7%. Khorvash et al. (2010) observed that H₂O₂ removed acid-insoluble lignin from soybean straw more effectively than treatment based on sodium hypochlorite, which suggested that bleaching with H₂O₂ improved the *in vitro* digestibility of soybean straw. Song et al. (2016) also reported that the acid-insoluble lignin content decreased in bamboo pretreated with alkali hydrogen peroxide. This behavior was attributed to the oxidation of lignin structures by products from H₂O₂ decomposition, such as hydroxyl radicals (HO$^-$) and superoxide anion radicals (O₂$^{-\bullet}$).

#### 3.1.2. Particle size and fiber morphology by SEM

Chemical treatment removed hemicelluloses and lignin from the fibers, resulting in particles with different size and highly reactive surfaces as compared to untreated soybean straw (Table 1). Soybean straw (SS) treated with NaOH and H₂O₂ tended to present large particle size (T4 = 122 μm and T3 = 145 μm), whereas SS treated with NaOH and NaClO₂ had smaller average particle size (T2 = 88 μm and T1 = 108 μm). However, we did not verify significant morphological differences. This behavior is in agreement with the behavior described by Brígida, Calado, Gonçalves, and Coelho (2010) when they treated coconut fibers. Larger particle size could indicate formation of agglomerates during mild treatment, as in the case when H₂O₂ was used as reactive bleaching agent. As previously discussed, NaOH associated with H₂O₂ removed lignin the most efficiently. The oxidation of lignin structures by H₂O₂ yielded fibers in which more hydroxyl groups were available for hydrogen inter-chain bonding, so the particles were more prone to agglomeration. This was mainly a result of their softer cationic potential (Brígida et al., 2010; Song et al., 2016).

Fig. 2 shows the SEM micrographs of untreated and chemically treated (T1, T2, T3, and T4) SS. The untreated fiber contained several cellulose microfibrils organized in a highly ordered parallel fashion featuring particles in a tightly packed conformation (Fig. 2A). Nontreated SS possessed a higher average particle diameter ($\sim$100 μm) as compared to chemically treated SS, which in turn presented isolated microfibrils in a free conformation with different dimen-
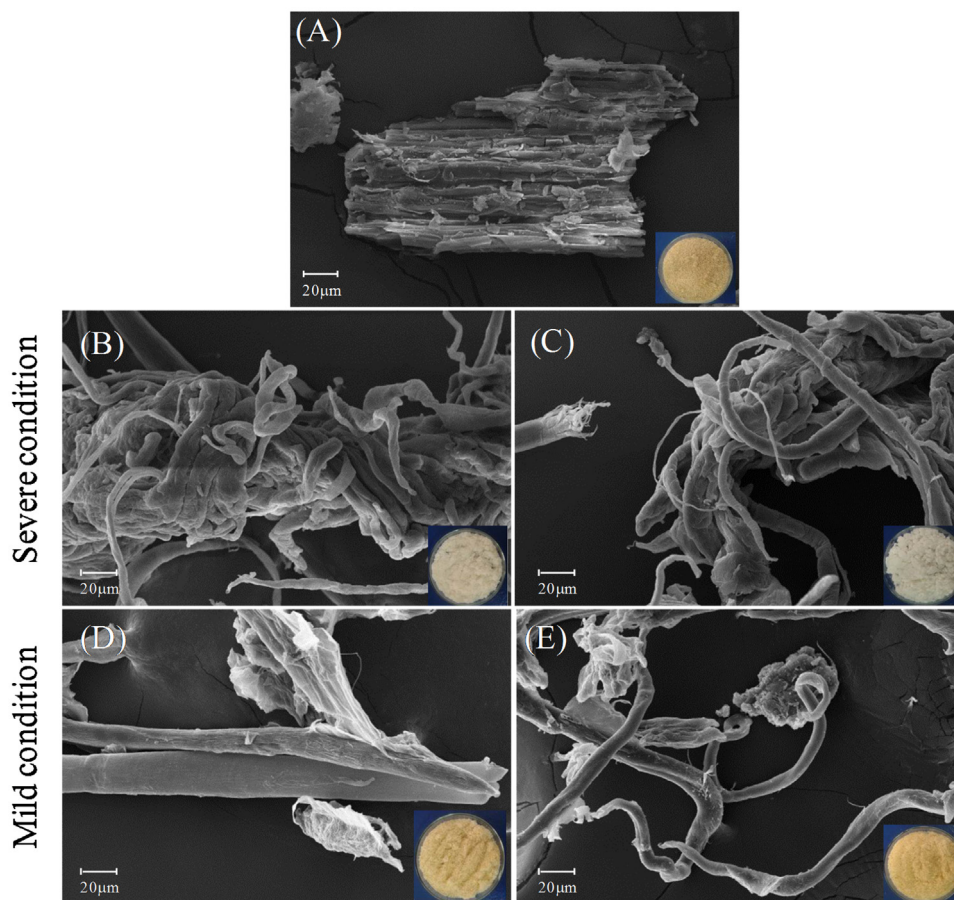
**Fig. 2.** SEM micrographs of (A) untreated soybean straw and of soybean straw after the different chemical treatments (B) T1, (C) T2, (D) T3, and (E) T4.

sions (diameters ranging from 0.4 to 10 μm and several microns in length) (Figs. 2B–E), a result of the reduced lignin and hemicelluloses content promoted by the chemical treatments (Table 1). The alkali treatments with $H_2O_2$ or $NaClO_2$ modified the morphology of the fiber by destroying some cell tissues and reducing the connections between the cells, a consequence of the partial removal of the external non-cellulosic layer composed of hemicelluloses, lignin, wax, and other impurities (Kallel et al., 2016). The bleaching step opened and subsequently defibrillated SS, which has a tendency to agglomerate into bundles. This confirmed the larger particle size measured for the samples SS-T3 and SS-T4.

### 3.1.3. XRD analysis of fiber crystallinity

Fig. 3 presents the diffraction patterns of untreated and chemically treated SS. The patterns were typical of semicrystalline cellulosic materials with an amorphous broad band and defined crystalline peaks. In all of the analyzed samples, the diffractogram profile indicated that cellulose type I predominated, with a main diffraction intensity at about $2\theta = 23°$ (plane 002) and identifiable peaks at $2\theta = 17°$ (plane 101) and 34° (plane 004). In cellulose I, the crystalline structure consists of two coexisting crystal phases: cellulose Iα (triclinic unit cell) and cellulose Iβ (monoclinic unit cell), which are arranged in parallel chains (Nishiyama, Langan, & Chanzy, 2002). The cellulose microfibrils impart crystallinity to the fibers because hemicelluloses and lignin are amorphous compounds.

In samples treated with higher concentrations of alkali (T2 and T4), the resulting crystalline structure consisted of a mixture of polymorphs of cellulose I and cellulose II. The typical diffractions peaks at $2\theta = 12°$ (plane 101), 20° (plane 101), and 22° (plane 002)
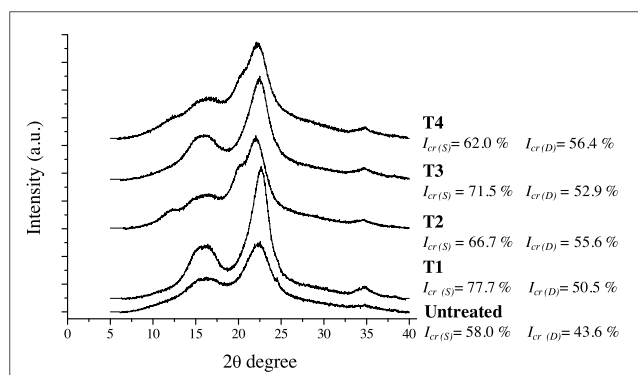


**Fig. 3.** X-ray diffractograms and crystalline index of untreated SS and treated SS samples (T1, T2, T3, and T4) as estimated by the Segal equation-XRD peak height ($I_{cr(S)}$) and by the XRD deconvolution method ($I_{cr(D)}$).

confirmed the presence of cellulose type II (Kafle, Greeson, Lee, & Kim, 2014; Yue et al., 2015). The main difference between cellulose allomorphs is the structure of their unit cell: in cellulose type I, the cellulose molecules are aligned in parallel, whilst the crystals are arranged in an antiparallel fashion in cellulose type II. Cellulose II has a more stable structure and can originate from treatment with alkali (Flauzino Neto, Silverio, Dantas, & Pasquini, 2013; Kafle et al., 2014; Yue et al., 2015) or from re-precipitation after hydrolysis in concentrated solution of sulfuric acid (Flauzino Neto et al., 2013; Silva & D'Almeida, 2009). Because bleaching treatments alone cannot generate cellulose type II, modifications to the
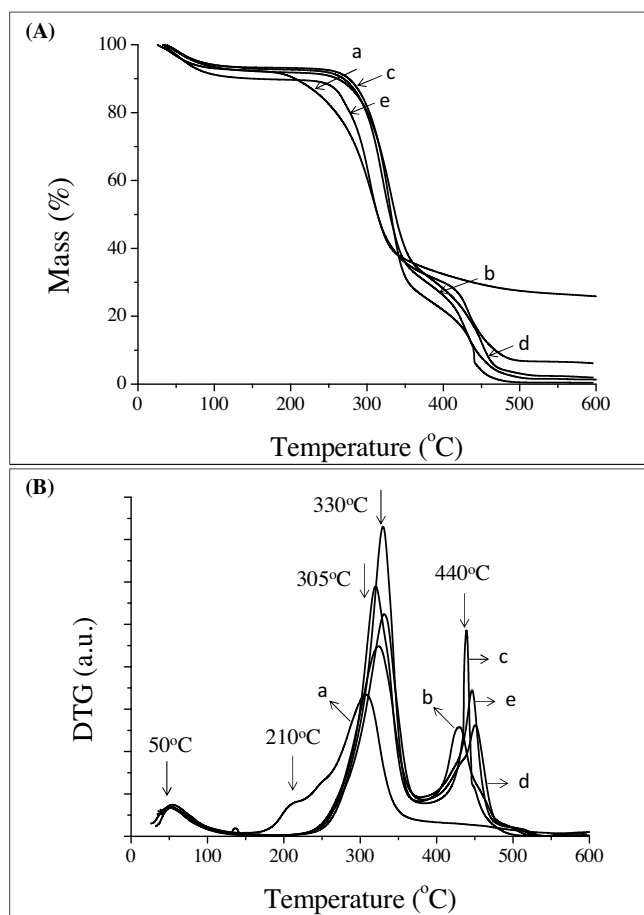
**Fig. 4.** (A) TGA and (B) DTG scans of (a) untreated soybean straw and soybean straw after chemical treatments (b) T1, (c) T2, (d) T3, and (e) T4, as described in Fig. 1.



**Fig. 5.** ATR-FTIR spectra of untreated soybean straw (untreated) and after chemical treatments T1, T2, T3, and T4.

crystalline structure of cellulose stem mainly from the higher concentrations of alkali (Song et al., 2016).

The resulting crystallinity indexes are presented alongside the curves. The methods used to estimate the crystallinity index ($I_{cr(S)}$ or $I_{cr(D)}$) afforded different values (Fig. 3). The method based on the height of the XRD peak height gave higher $I_{cr}$ than the method based on deconvolution of the XRD peak. Ground soybean straw presented $I_{cr(S)}$ of 58%, which agreed with values reported in the literature (Alemdar & Sain, 2008) for the crystallinity of native cellulose estimated by the Segal equation (Park et al., 2010). Conversely, the method based on deconvolution of the XRD peak has been widely used to analyze the structure of cellulose II structure because the Segal relation does not take some peaks (12° and 20°) into account. The XRD deconvolution method is therefore considered more appropriate to compare the treatments applied to SS.

For the chemically treated samples, the crystalline fraction increased as the amorphous constituents were removed. $I_{cr(D)}$ ranged from 43.6% (untreated samples) up to 56.4% (samples T4). The different treatments gave $I_{cr(D)}$ values that decreased in the following order: T4 ≥ T2 > T3 > T1 > Untreated samples. The XRD results agreed with the chemical composition (Table 1): samples with higher cellulose and lower hemicellulose contents (T2 and T4) had higher crystallinity. These samples were treated with high concentration of NaOH, and the bleaching agent apparently did not affect these results.

### 3.1.4. Thermal stability of the fiber

Fig. 4A and B displays the thermogravimetric analysis (TGA) and the corresponding derivative (DTG) curves of SS, respectively.
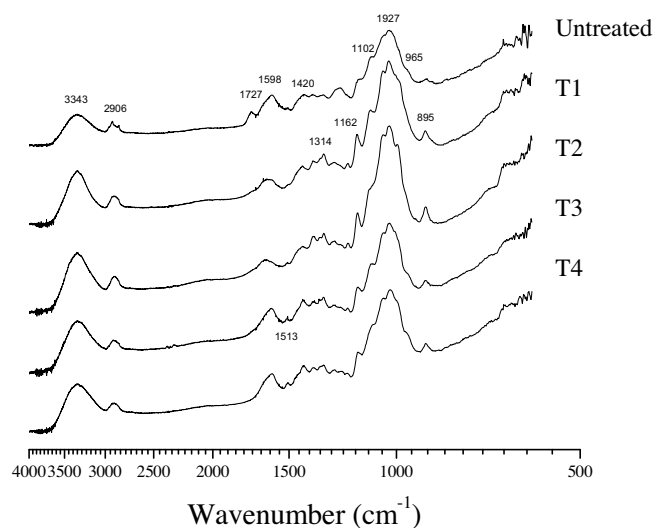
Untreated SS presented two distinct decomposition events. The first, with maximum intensity at 50 °C, mass loss of 7.6%, corresponded to desorption of physically and chemically bound water and volatiles. The second event occurred between 230 and 350 °C, with maximum at 305 °C, and referred to the thermo-oxidative reaction of the main organic compounds (decomposition of lignin, hemicelluloses, and mainly cellulose) with overall mass loss around 60%. The shoulder identified at 210 °C in the DTG curve (Fig. 4B) was considered the start of hemicellulose degradation (Antal & Varhegyi, 1995). At temperatures higher than 400 °C, the weight dropped significantly, generating solid residues such as ashes and inorganic materials (around 20% of the initial mass).

For the first mass loss event, the treated samples presented similar mass loss values (7.3%), except for SS treated with NaOH 17.5% and $H_2O_2$ (T4), which experienced mass loss of 10.1%. Higher exposure of cellulose probably accounted for this observation, as reported by Brígida et al. (2010) and Silva, Souza, Machado, and Hourston (2000). Consequently, these samples presented cellulose with higher crystallinity, as observed by SEM and XRD. Moreover, the chemical treatments changed the thermal characteristics and degradation of the lignocellulose materials. The initial mass loss was followed by a narrower and more marked event with maximum centered around 330 °C, primarily attributed to degradation of cellulose (Rosa et al., 2009). For the treated samples, this main decomposition event shifted to higher temperatures due to previous chemical removal of part of the hemicelluloses present in the fibers (Table 1), which increased the thermal stability of the fiber (Bismarck et al., 2001; Brígida et al., 2010; Rosa et al., 2009). At this stage, the average mass loss was 68%, which was ascribed to degradation of hemicellulose and cellulose given that this figure was not far from the measured fraction of hemicelluloses plus cellulose found in the treated samples (Table 1).

The third additional event (not observed for raw ground materials) occurred from 380 to 500 °C, with maximum at 440 °C. It was ascribed solely to the degradation of lignin (the most stable of the three compounds). Above this temperature, pyrolysis occurred, which was associated with release of carbon dioxide and consequent reduction of the residual mass.

### 3.1.5. ATR-FTIR spectroscopy

As previously discussed, the chemical composition of the fibers varied depending on the applied treatment. Comparison between the infrared spectra of untreated and treated fibers (Fig. 5) helped

**Table 2**
Mechanical properties, moisture, solubility in water, and water vapor permeability (WVP) of SPI/soybean straw composite films.

| Film[*] | Thickness (μm) | Tensile strength (MPa) | Elongation at break (%) | Young's modulus (MPa) | Moisture (%) | Solubility in water (%) | WVP ($10^{-10}$ g/msPa) |
|---|---|---|---|---|---|---|---|
| SPI | 55 ± 11[c] | 5.6 ± 0.7[cd] | 30 ± 9[ab] | 298 ± 52[c] | 15.3 ± 0.5[a] | 63 ± 5[a] | 12.2 ± 0.2[a] |
| SPI/soybean straw (untreated) | 66 ± 13[bc] | 4.6 ± 0.4[d] | 35 ± 12[b] | 270 ± 31[c] | 15.9 ± 0.4[a] | 61 ± 9[a] | 9.8 ± 1.2[a] |
| SPI/soybean straw T1 | 63 ± 11[bc] | 7.1 ± 0.7[b] | 20 ± 5[ac] | 392 ± 32[b] | 13.2 ± 0.2[bc] | 44 ± 6[ab] | 10.9 ± 1.5[a] |
| SPI/soybean straw T2 | 81 ± 17[ab] | 5.8 ± 0.6[c] | 18 ± 6[c] | 314 ± 19[c] | 12.8 ± 0.5[b] | 45 ± 7[ab] | 9.9 ± 1.6[a] |
| SPI/soybean straw T3 | 83 ± 16[ab] | 9.0 ± 0.7[a] | 15 ± 5[c] | 521 ± 72[a] | 14.1 ± 0.1[c] | 46 ± 4[b] | 11.0 ± 1.0[a] |
| SPI/soybean straw T4 | 60 ± 11[c] | 7.8 ± 0.8[b] | 17 ± 5[c] | 527 ± 37[a] | 13.4 ± 0.4[bc] | 36 ± 3[b] | 12.8 ± 2.1[a] |

[a–e]Means with different superscript letters in the same column are statistically different (Fisher, $p < 0.05$).

[*] All formulations contained 5% SPI (w/w), and the added untreated soybean straw or chemically treated soybean straw (T1, T2, T3 and T4) corresponded to 1% (g/100 g of SPI).

to identify some variations. All the spectra were rather similar, indicating that an analogous structure predominated in all the samples. In general, the spectra were representative of the vibrational patterns of polysaccharides with bands typically assigned to cellulose and hemicelluloses and which have been widely interpreted in the literature. A common broad band centered at 3343 cm⁻¹ corresponded to the stretching vibration of −OH groups, which is common in hydrophilic materials. The peaks identified at around 2906 cm⁻¹ referred to symmetric and asymmetric CH group stretching. According to Andrade-Mahecha et al. (2015), these peaks indicate the presence of lignin. A small band at 1727 cm⁻¹ (best observed in the spectrum of the untreated SS) was attributed to the carbonyl groups of the uronic ester groups of hemicelluloses or to the ester linkage of the carboxylic group of the ferulic and p-coumeric acids of lignin and/or hemicelluloses (Alemdar & Sain, 2008; Andrade-Mahecha et al., 2015). This band diminished or even disappeared in the treated samples, indicating that the chemical treatments removed lignin and hemicelluloses, in accordance to the chemical composition shown in Table 1. The peak at 1598 cm⁻¹ was strongly associated with the CO stretching mode of the lignin aromatic ring. A reduction in its intensity and/or its shift to higher wavelengths was related to scission or modification of the aromatic ring and corresponded to delignification (Li et al., 2010).

The multiple absorbance peaks between 1420 and 1162 cm⁻¹ were due to typical vibrations of primary and secondary hydroxyl bending in cellulose (Liu, Yu, & Huang, 2005). The peaks in the region between 1102 and 965 cm⁻¹ referred to CH, HCH, and OCH deformation. The most intense peak centered at 1927 cm⁻¹ was assigned to CH asymmetric vibration of cellulose. This peak became sharper after the treatments, particularly in the case of T2, which was the treatment that yielded the most cellulose. The most readily identifiable differences among the samples was the band at 1162 cm⁻¹, corresponding to the asymmetric stretching of the C-O-C glycoside and C-O-C β-1,4 glycosyl linkage of cellulose (Liu, Yu et al., 2005; Michell, 1990). These differences were clearly evident in the spectra of the fibers resulting from the more severe treatments (T1 and T2). Additionally, the peak centered at 895 cm⁻¹ was ascribed to the glycosidic linkages of the glucose ring in cellulose (Alriols, Blanco, Mondragon, & Labidi, 2009; Chirayil et al., 2014). This peak emerged in the spectra of all the samples. In the untreated SS, this peak overlapped with the broad peak due to CH deformation (centered at 1927 cm⁻¹) of the structure of cellulose. The treatments defibrillated cellulose. Consequently, the bands narrowed and became more defined, allowing for better visualization of the contribution of the remaining hemicelluloses.

### 3.2. SPI/soybean straw composite films: mechanical and physical properties

Table 2 summarizes the mechanical properties (tensile strength, elongation at break, and Young's modulus), moisture, solubility in water, and water vapor permeability (WVP) of SPI films con-

taining untreated and chemically treated SS. The thickness of the SPI/soybean straw composite films ranged from 60 to 83 μm. Addition of untreated SS to the soy protein films did not improve the mechanical properties of the film. However, incorporation of chemically treated fibers into SPI films promoted higher tensile strength (TS) and Young's modulus (YM), but lower elongation at break (EB) as compared to the control film. This effect was more evident when soybean straw submitted to T3 was added to the film. In this case, TS increased from 5.6 ± 0.7 to 9.0 ± 0.7 MPa, YM rose from 298 ± 52 MPa to 521 ± 72 MPa, and elongation at break decreased by 50% (from 30 to 15%). Addition of SS treated by T1 and T4 had practically the same effect on the mechanical properties, except that T4 improved the YM values more significantly, as reflected on the stiffness of the film. Fibers treated with different concentrations of NaOH (1% or 2%) and pure cellulose fibers improved the mechanical properties of fiber-reinforced composites significantly (Cho, Skrifvars, Hemanathan, Mahimaisenan, & Adekunle, 2014). Liu, Misra, Askeland, Drzal, and Mohanty (2005) verified the same result when they evaluated Indian grass fibers treated with high concentration of alkali as filler in soy-based biocomposites.

The removal of hemicelluloses by alkali treatment and the removal of lignin by bleaching reaction can favor the formation of intermolecular hydrogen bonds between the hydroxyl and carbonyl groups of the SPI matrix with the hydroxyl groups of the treated SS, to yield a network with better mechanical resistance (Husseinsyah et al., 2014).

Incorporation of untreated SS did not modify the solubility or the moisture content of composite films. Compared to the control, composite films containing chemically treated SS had lower moisture and solubility. Addition of treated fibers reduced both the solubility and the moisture content by around 42% and 13%, respectively, because stronger bonds probably emerged between the hydroxyl and carbonyl groups of the SPI matrix and the hydroxyl groups of treated SS. SPI contains many polar amino acids, which results in films that are more susceptible to high moisture (Yarin, Pourdeyhimi, & Ramakrishna, 2014). The added treated SS could interact with these groups, to decrease the water affinity of the matrix. Water can act as plasticizer, and the presence of fewer water molecules in a SPI/SS composite reduces the elongation at break of these films, as observed in Table 2. Reduction in the amount of hydrophilic groups available to bind with the water molecules renders a more stable three-dimensional network. Addition of SS-T4 to the SPI film led to the lowest solubility because this soybean straw sample had the lowest content of hemicelluloses and insoluble lignin (Table 1). Kumar, Choudhary, Mishra, and Varma (2008) reported similar results for water affinity after they introduced alkali-treated banana fibers into an SPI matrix.

Addition of 1% (w/w) of fibers as reinforcing filler did not reduce WVP as expected. Although the presence of fibers in the matrix usually increase tortuosity and consequently reduce film permeability (Jensen et al., 2015), the amount of fibers added herein did not change the permeability significantly as judged from the

results of Tukey's test (p > 0.05) summarized in Table 2. Permeability strongly depends on film porosity. The irregular incorporation of cellulose fibers into protein films could generate internal cracks and pores, as reported by Pereda, Amica, Rácz, and Marcovich (2011) for caseinate-based films reinforced with cellulose fibers. During the drying process, fibers can act as nucleation sites where bubbles can grow, reducing the water vapor barrier properties.

## 4. Conclusions

Chemical treatments of soybean straw including reaction with alkali and bleaching yielded materials with higher cellulose content as confirmed by TGA and FTIR analysis. The cellulose content in the fibers was attributed to effective removal of hemicelluloses, lignin, and other inert and inorganic materials. The degree of cellulose crystallinity was increased as the amorphous constituents were removed during the treatments. During these treatments, the use of high concentration of NaOH contributed to the allomorph transition from cellulose I to II, regardless of the bleaching agent. These specific differences can influence the application of the resulting fibers. The treated SS performed better as reinforcement filler in SPI films. The filler increased the mechanical resistance of the film because it promoted stronger interactions between the polar groups in the protein and the hydroxyl functionalities in the treated fibers. The soybean straw treated with hydrogen peroxide affected both the mechanical properties and the solubility of the film, mainly due to the removal of lignin. The addition of 1% of fibers did not modify the water vapor permeability of the film significantly. Different percentages of fillers should be evaluated for an effective reduction in WVP values.

## Acknowledgments

## References

ASTM D882-95. (1995). *Standard test method for tensile properties of thin plastic sheeting. Annual book of ASTM standards*. Philadelphia: American Society for Testing and Materials.

ASTM E96-95. (1995). *Standard method for water vapor transmission of materials. Annual book of ASTM standards*. Philadelphia: American Society for Testing and Materials.

Alemdar, A., & Sain, M. (2008). Isolation and characterization of nanofibers from agricultural residues—Wheat straw and soy hulls. *Bioresource Technology*, 99(6), 1664–1671.

Alriols, M. G., Blanco, T. M., Mondragon, I., & Labidi, J. (2009). Agricultural palm oil tree residues as raw material for cellulose, lignin and hemicelluloses production by ethylene glycol pulping process. *Chemical Engineering Journal*, 148(1), 106–114.

Andrade-Mahecha, M. M., Pelissari, F. M., Tapia-Blácido, D. R., & Menegalli, F. C. (2015). Achira as a source of biodegradable materials: Isolation and characterization of nanofibers. *Carbohydrate Polymers*, 123(0), 406–415.

Antal, M. J., & Varhegyi, G. (1995). Cellulose pyrolysis kinetics—The current state knowledge. *Industrial & Engineering Chemistry Research*, 34(3), 703–717.

Bismarck, A., Mohanty, A. K., Aranberri-Askargorta, I., Czapla, S., Misra, M., Hinrichsen, G., et al. (2001). Surface characterization of natural fibers; surface properties and the water up-take behavior of modified sisal and coir fibers. *Green Chemistry*, 3(2), 100–107.

Bose, M. L. V., & Martins Filho, J. G. (1984). O papel dos resíduos agroindustriais na alimentação de ruminantes. *Informe Agropecuário*, 10(119), 3–7.

Brígida, A. I. S., Calado, V. M. A., Gonçalves, L. R. B., & Coelho, M. A. Z. (2010). Effect of chemical treatments on properties of green coconut fiber. *Carbohydrate Polymers*, 79(4), 832–838.

CONAB. Companhia Nacional de Abastecimento. (2015). *Monitoring of the Brazilian grain hasvest 2015/2016*. Available online http://www.conab.gov.br Accessed 15.02.16

Cabrera, E., Muñoz, M. J., Martín, R., Caro, I., Curbelo, C., & Díaz, A. B. (2015). Comparison of industrially viable pretreatments to enhance soybean straw biodegradability. *Bioresource Technology*, 194, 1–6.

Calabria, L., Vieceli, N., Bianchi, O., Boff de Oliveira, R. V., do Nascimento Filho, I., & Schmidt, V. (2012). Soy protein isolate/poly(lactic acid) injection-molded biodegradable blends for slow release of fertilizers. *Industrial Crops and Products*, 36(1), 41–46.

Campos, A., Correa, A. C., Cannella, D., Teixeira, E. M., Marconcini, J. M., Dufresne, A., et al. (2013). Obtaining nanofibers from curauá and sugarcane bagasse fibers using enzymatic hydrolysis followed by sonication. *Cellulose*, 20, 1491–1500.

Chan, R., Lim, L. T., Barbut, S., & Marcone, M. F. (2014). Extrusion and characterization of soy protein film incorporated with soy cellulose microfibers. *International Polymer Processing*, 29(4), 467–476.

Chen, P., Zhang, L. N., Peng, S. P., & Liao, B. (2006). Effects of nanoscale hydroxypropyl lignin on properties of soy protein plastics. *Journal of Applied Polymer Science*, 101(1), 334–341.

Chirayil, C. J., Joy, J., Mathew, L., Mozetic, M., Koetz, J., & Thomas, S. (2014). Isolation and characterization of cellulose nanofibrils from Helicteres isora plant. *Industrial Crops and Products*, 59, 27–34.

Cho, S. W., Skrifvars, M., Hemanathan, K., Mahimaisenan, P., & Adekunle, K. (2014). Regenerated cellulose fibre reinforced casein films: Effect of plasticizer and fibres on the film properties. *Macromolecular Research*, 22(7), 701–709.

Deepa, B., Abraham, E., Cherian, B. M., Bismarck, A., Blaker, J. J., Pothan, L. A., et al. (2011). Structure, morphology and thermal characterisitics of banana nano fibers obtained by steam explosion. *Bioresource Technology*, 102(2), 1988–1997.

Denavi, G., Tapia-Blacido, D. R., Anon, M. C., Sobral, P. J. A., Mauri, A. N., & Menegalli, F. C. (2009). Effects of drying conditions on some physical properties of soy protein films. *Journal of Food Engineering*, 90(3), 341–349.

FAOSTAT. Food and Agriculture Organization of United Nations (2016). Production, Crops, Soybeans. Available online http://faostat.fao.org/ Accessed 10.08.16.

Flauzino Neto, W. P., Silverio, H. A., Dantas, N. O., & Pasquini, D. (2013). Extraction and characterization of cellulose nanocrystals from agro-industrial residue—Soy hulls. *Industrial Crops and Products*, 42, 480–488.

Garrido, T., Peñalba, M., de la Caba, K., & Guerrero, P. (2016). Injection-manufactured biocomposites from extruded soy protein with algae waste as a filler. *Composites Part B: Engineering*, 86, 197–202.

González, A., Strumia, M. C., & Alvarez Igarzabal, C. I. (2011). Cross-linked soy protein as material for biodegradable films: Synthesis, characterization and biodegradation. *Journal of Food Engineering*, 106(4), 331–338.

Husseinsyah, S., Yeng, C. M., Kassim, A. R., Zakaria, M. M., & Ismail, H. (2014). Kapok husk-reinforced soy protein isolate biofilms: Tensile properties and enzymatic hydrolysis. *BioResources*, 9(3), 5636–5651.

Jensen, A., Lim, L. T., Barbut, S., & Marcone, M. (2015). Development and characterization of soy protein films incorporated with cellulose fibers using a hot surface casting technique. *LWT—Food Science and Technology*, 60(1), 162–170.

Kafle, K., Greeson, K., Lee, C., & Kim, S. H. (2014). Cellulose polymorphs and physical properties of cotton fabrics processed with commercial textile mills for mercerization and liquid ammonia treatments. *Textile Research Journal*, 84(16), 1692–1699.

Kafle, K., Lee, C. M., Shin, H., Zoppe, J., Johnson, D. K., Kim, S. H., et al. (2015). Effects of delignification on crystalline cellulose in lignocellulose biomass characterized by vibrational sum frequency generation spectroscopy and X-ray diffraction. *Bioenergy Resource*, 8(4), 1750–1758.

Kallel, F., Bettaieb, F., Khiari, R., García, A., Bras, J., & Chaabouni, S. E. (2016). Enzyme Isolation and structural characterization of cellulose nanocrystalsextracted from garlic straw residues. *Industrial Crops and Products*, 87, 287–296.

Khorvash, M., Kargar, S., Yalchi, T., & Ghorbani, G. R. (2010). Effects of hydrogen peroxide and sodium hypochlorite on the chemical composition and in vitro digestibility of soybean straw. *Journal of Food Agriculture & Environment*, 8(3&4), 848–851.

Kim, J. T., & Netravali, A. N. (2012). Physical properties of biodegradable films of soy protein concentrate/gelling agent blends. *Macromolecular Materials and Engineering*, 297(2), 176–183.

Kumar, R., Choudhary, V., Mishra, S., & Varma, I. (2008). Banana fiber reinforced biodegradable soy protein composites. *Frontiers of Chemistry in China*, 3(3), 243–250.

Li, C., Knierim, B., Manisseri, C., Arora, R., Scheller, H. V., Auer, M., et al. (2010). Comparison of dilute acid and ionic liquid pretreatment of switchgrass: Biomass recalcitrance, delignification and enzymatic saccharification. *Bioresource Technology*, 101(13), 4900–4906.

Liu, W., Misra, M., Askeland, P., Drzal, L. T., & Mohanty, A. K. (2005). 'Green' composites from soy based plastic and pineapple leaf fiber: Fabrication and properties evaluation. *Polymer*, 46, 2710–2721.

Liu, R., Yu, H., & Huang, Y. (2005). Structure and morphology of cellulose in wheat straw. *Cellulose*, 12(1), 25–34.

Lodha, P., & Netravali, A. N. (2002). Characterization of interfacial and mechanical properties of green composites with soy protein isolate and ramie fiber. *Journal of Materials Science*, 37(17), 3657–3665.

Michell, A. J. (1990). Second-derivative F.t.-i.r. spectra of native celluloses. *Carbohydrate Research*, 197(0), 53–60.

Milazzo, M. F., Spina, F., Cavallaro, S., & Bart, J. C. J. (2013). Sustainable soy biodiesel. *Renewable and Sustainable Energy Reviews*, 27, 806–852.

Nishiyama, Y., Langan, P., & Chanzy, H. (2002). Crystal structure and hydrogen-bonding system in cellulose Ibeta from synchrotron X-ray and

neutron fiber diffraction. *Journal of the American Chemical Society, 124*(31), 9074–9082.

Oh, Y. H., Eom, I. Y., Joo, J. C., Yu, J. H., Song, B. K., Lee, S. H., et al. (2015). Recent advances in development of biomass pretreatment technologies used in biorefinery for the production of bio-based fuels, chemicals and polymers. *Korean Journal of Chemical Engineering, 32*(10), 1945–1959.

Park, S., Baker, J. O., Himmel, M. E., Parilla, P. A., & Johnson, D. K. (2010). Cellulose crystallinity index: Measurement techniques and their impact on interpreting cellulase performance. *Biotechnology for Biofuels, 3*, 1–10.

Pereda, M., Amica, G., Rácz, I., & Marcovich, N. E. (2011). Structure and properties of nanocomposite films based on sodium caseinate and nanocellulose fibers. *Journal of Food Engineering, 103*(1), 76–83.

Reddy, N., & Yang, Y. (2009). Natural cellulose fibers from soybean straw. *Bioresource Technology, 100*, 3593–3598.

Rosa, M. F., Chiou B.-s. Medeiros, E. S., Wood, D. F., Williams, T. G., Mattoso, L. H. C., Orts, W. J., et al. (2009). Effect of fiber treatments on tensile and thermal properties of starch/ethylene vinyl alcohol copolymers/coir biocomposites. *Bioresource Technology, 100*(21), 5196–5202.

Saenghirunwattana, P., Noomhorm, A., & Rungsardthong, V. (2014). Mechanical properties of soy protein based green composites reinforced with surface modified cornhusk fiber. *Industrial Crops and Products, 60*, 144–150.

Satyanarayana, K. G., Arizaga, G. G. C., & Wypych, F. (2009). Biodegradable composites based on lignocellulosic fibers—An overview. *Progress in Polymer Science, 34*(9), 982–1021.

Segal, L., Creely, J. J., Martin, A. E., & Conrad, C. M. (1959). An empirical method for estimating the degree of crystallinity of native cellulose using the X-Ray diffractometer. *Textile Research Journal, 29*, 786–794.

Silva, D. J., & D'Almeida, M. L. O. (2009). Nanocristais de celulose—Cellulose whiskers. *O Papel, 70*, 34–52.

Silva, G. C., Souza, D. A., Machado, J. C., & Hourston, D. J. (2000). Mechanical and thermal characterization of native Brazilian coir fiber. *Journal of Applied Polymer Science, 76*, 1197–1206.

Siro, I., & Plackett, D. (2010). Microfibrillated cellulose and new nanocomposite materials: A review. *Cellulose, 17*(3), 459–494.

Song, X., Jiang, Y., Rong, X., Wei, W., Wang, S., & Nie, S. (2016). Surface characterization and chemical analysis of bamboo substrates pretreated by alkali hydrogen peroxide. *Bioresource Technology, 216*, 1098–1101.

Sun, L., Chen, W. S., Liu, Y. X., Li, J., & Yu, H. P. (2015). Soy protein isolate/cellulose nanofiber complex gels as fat substitutes: Rheological and textural properties and extent of cream imitation. *Cellulose, 22*(4), 2619–2627.

Sun, J. (2004). Isolation and characterization of cellulose from sugarcane bagasse. *Polymer Degradation and Stability, 84*(2), 331–339.

TAPPI (1991). TAPPI Standard. – Method T19 om-54. *TAPPI Test Methods*.

TAPPI (1999). TAPPI Standard. – Method T222 om-88. *TAPPI Test Methods*.

Tapia-Blácido, D., Sobral, P., & Menegalli, F. (2011). Optimization of amaranth flour films plasticized with glycerol and sorbitol by multi-response analysis. *LWT—Food Science and Technology, 44*(8), 1731–1738.

Wan, C., Zhou, Y., & Li, Y. (2011). Liquid hot water and alkaline pretreatment of soybean straw for improving cellulose digestibility. *Bioresource Technology, 102*(10), 6254–6259.

Wang, Y. X., Cao, X. D., & Zhang, L. N. (2006). Effects of cellulose whiskers on properties of soy protein thermoplastics. *Macromolecular Bioscience, 6*(7), 524–531.

Wang, Y., Mo, X., Sun, X. S., & Wang, D. H. (2007). Soy protein adhesion enhanced by glutaraldehyde crosslink. *Journal of Applied Polymer Science, 104*(1), 130–136.

Wei, M., Fan, L. H., Huang, J., & Chen, Y. (2006). Role of star-like hydroxylpropyl lignin in soy-protein plastics. *Macromolecular Materials and Engineering, 291*(5), 524–530.

Won, J. S., Lee, J. E., Jin, D. Y., & Lee, S. G. (2015). Mechanical properties and biodegradability of the kenaf/soy protein isolate-PVA biocomposites. *International Journal of Polymer Science*,. Article ID 860617, 11p

Xiao, B., Sun, X. F., & Sun, R. C. (2001). Chemical, structural, and thermal characterizations of alkali-soluble lignins and hemicelluloses, and cellulose from maize stems, rye straw, and rice straw. *Polymer Degradation and Stability, 74*(2), 307–309.

Xu, Z., Wang, Q., Jiang, Z. H., Yang, X., & Ji, Y. (2007). Enzymatic hydrolysis of pretreated soybean straw. *Biomass and Bioenergy, 31*, 162–167.

Xu, F., Dong, Y., Zhang, W., Zhang, S., Li, L., & Li, J. (2015). Preparation of cross-linked soy protein isolate-based environmentally-friendly films enhanced by PTGE and PAM. *Industrial Crops and Products, 67*, 373–380.

Yarin, A. L., Pourdeyhimi, B., & Ramakrishna, S. (2014). *Fundamentals and applications of micro- and nanofibers*. United Kingdom: Cambridge University Press.

Yue, Y., Han, J., Han, G., Zhang, Q., French, A. D., & Wu, Q. (2015). Characterization of cellulose I/II hybrid fibers isolated from energycane bagasse during the delignification process: Morphology, crystallinity and percentage estimation. *Carbohydrate Polymers, 133*, 438–447.

Zeronian, S. H., & Inglesby, M. K. (1995). Bleaching of cellulose by hydrogen peroxide. *Cellulose, 2*(4), 265–272.